SCIENTIFIC REPORTS
nature research

OPEN

Nintedanib ameliorates animal model of dermatitis

Min-Jeong Heo[1], Chanmi Lee[1], Soo Young Choi[1], Yeong Min Choi[1], In-sook An[1], Seunghee Bae[2], Sungkwan An[2*] & Jin Hyuk Jung[1*]

Nintedanib, a receptor tyrosine kinase (RTK) inhibitor has been developed as therapeutics for idiopathic pulmonary fibrosis and non-small lung cancer. We found that the expression levels of RTK, especially VEGFR1 is increased in skin biopsies of dermatitis patients from multiple independent datasets. Moreover, VEGFR1 is highly expressed by infiltrated cells in dermis from oxazolone (OXA) treated mice. Interestingly, nintedanib alleviates dermatitis symptom in OXA-induced animal model. Especially, levels of epidermis thickness, infiltrated immune cells including mast cells and eosinophils were decreased from mice cotreated with nintedanib and OXA compared with OXA treated mice. Moreover, serum IgE and Th2 cytokines including IL-4 and IL-13 were decreased by nintedanib treatment. These results suggest an evidence that nintedanib alleviates animal model of dermatitis.

Receptor tyrosine kinases (RTKs) are membrane bound receptors for growth factors and hormones that modulate cellular process to have a crucial role in the development[1,2]. Because RTKs also often overexpressed in cancers including breast and non-small lung cancers, many inhibitors against RTKs have been developed for anticancer treatments[3]. On the other hands, tyrosine kinase mediates the signal from various immune related receptors including leukocyte antigen receptors, innate immune receptors, and cytokine receptors to activate immune cells and recruit to inflammation lesion[4]. Autoimmune and inflammatory diseases are characterized by inflammatory microenvironment and tyrosine kinase serves essential role in immune-mediated disorders[5]. Therefore, small molecules targeting tyrosine kinase have been developed for autoimmune and inflammatory diseases[6–8]. Especially JAK is a one of primary tyrosine kinases for therapeutic target since JAK is responsible for numerous cytokines expression via type I/II cytokine receptor signaling[9–11]. Many JAK inhibitors are FDA approved in clinic use for autoimmune and inflammatory diseases[12]. Atopic dermatitis (AD) is one of the most common skin inflammatory diseases affecting 3–10% adults and 15–20% of children in USA[13–15]. AD pathogenesis is a complex of skin barrier dysfunction, alteration of immune responses, IgE-mediated hypersensitivity[16,17]. Treatments of atopic dermatitis are non-specific immunosuppressants and Th2 specific therapies including biologics[18–20]. Because IL-4, which is a primary pathogenic in AD requires JAK1 and 3 with additional complex, JAK inhibitors including tofacitinib and baricitinib have been determined their efficacy on the AD[21–23]. VEGFR1 is a receptor of VEGF, transduces a signal to induce angiogenesis and lymphangiogenesis[24,25]. Dilated vessels and perivascular edema are frequently found in AD lesion with erythema[26,27]. Moreover, increased levels of VEGF are found in plasma and AD lesion[28,29]. Although VEGF-VEGFR signaling is highly activated in AD, use of VEGFR inhibitor for AD treatment remains unexplored. Interestingly, we found expression levels of RTKs are upregulated in skin biopsies of dermatitis patients from several independent datasets (Fig. 1 and Table S1). Nintedanib is a potent receptor kinase inhibitor that competitively binds to the kinase domains of vascular endothelial growth factor receptor (VEGFR), platelet-derived growth factor receptor beta (PDGFRB) and fibroblast growth factor receptor (FGFR)[30]. Nintedanib is a FDA-approved oral drug for idiopathic pulmonary fibrosis (IPF)[31]. Here we used nintedanib to determine whether nintedanib attenuates oxazolone-induced animal model of dermatitis.

Material and Methods

All methods were performed in accordance with the relevant guidelines and regulations.

Experimental animals. 7-week-old BALB/c mice were purchased from the Central Laboratory Animals (Seoul, Korea). They were feed and raised under specific pathogen-free conditions with 12 h light/dark cycle in controlled environment condition as temperature and humidity. All experimental procedures were approved by the Institutional Animal Care and Use Committee of the Konkuk University (KU19160).

[1]Korea Institute of Dermatological Science, GeneCellPharm Corporation, 375 Munjeong 2(i)-dong, Songpa-gu, Seoul, 05836, South Korea. [2]Research Institute for Molecular-Targeted Drugs, Department of Cosmetics Engineering, Konkuk University, Seoul, 05029, South Korea. *email: ansungkwan@konkuk.ac.kr; jungjh@skinreseach.or.kr

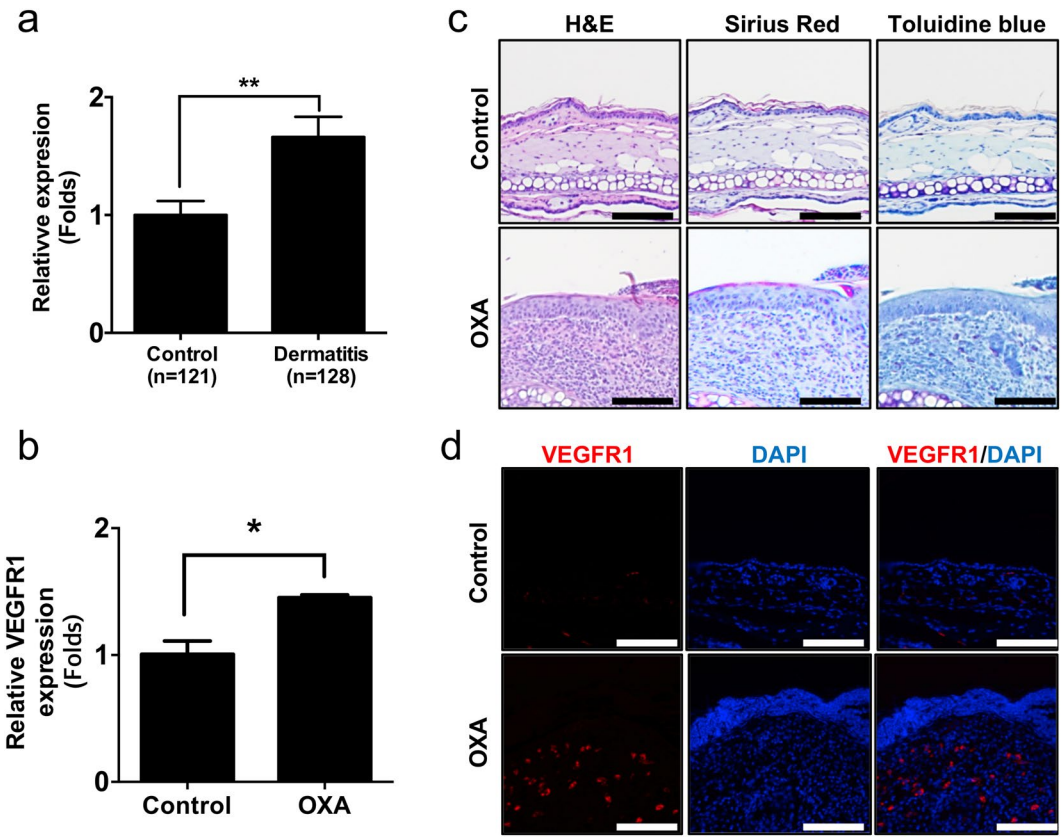

Figure 1. The expression levels of VEGFR1/*FLT1* in animal model of dermatitis and dermatitis patients. (**a**) Relative expression levels of *FLT1* in normal (n = 121) and dermatitis patients (n = 128). (**b**) mRNA expression of *Flt1* was measured in oxazolone (OXA) treated mice ear and vehicle control (n = 15). (**c**) Histological analysis (H&E, Sirius red and toluidine blue staining) of control and oxazolone treated mice ear. Scale bar = 100 μm. (**d**) Immunofluorescent analysis of VEGFR1 from control and oxazolone treated mice ear. Scale bar = 100 μm. Data are presented as mean ± SEM and analyzed by student t-test. *$p < 0.05$, **$p < 0.01$ compared to control.

OXA-induced murine model of dermatitis. To induce AD-like lesion, all ears of mice except the negative control group were applied with oxazolone (OXA). OXA-induced animal model of dermatitis was performed according to previously described with some modifications[32,33]. Briefly, skin inflammation was induced by topical administration with 30 μl of 1% OXA dissolved in acetone (Merck, Kenilworth, USA) on day 0, and repeated 30 μl of 0.2% OXA three times a week from day 7 to 21. Negative control group was treated same volume of vehicles. Therapeutic groups as 0.68 mg/kg dexamethasone (DEX) or 7 mg/kg Nintedanib (NIN) were applied on ear after 1 h every challenge. Drug administration was performed under light anesthesia with isoflurane. Detailed description is as shown Fig. 2a. Mice were photographed by Digital Single-Lens Reflex camera (Conditions; F5.6 1/40, ISO800; Canon, Tokyo, Japan).

Ear thickness and ear weight. Ear thickness was measured every other day using digital micrometer (Japan), and ear was collected using 5-mm biopsy punch (KAI Medical, Japan) after sacrifice for measuring weight on day 21.

Histology. Ear tissues were fixed in 10% formalin solution (Sigma, Mo, USA) for 24 h. Tissues were washed with PBS (Biosesang, Seongnam, Korea), embedded in paraffin (Leica Biosystems, Wetzlar, Germany) and sectioned 4 μm thickness using microtome (HistoCore BIOCUT; Leica Biosystems, Germany). Stained images were taken using light microscope (Olympus, Tokyo, Japan). Mast cells or eosinophils were counted in 3 random high-power field (HPF) each mouse at 400× magnification. H&E staining was performed according to previously described[34]. Epidermis and dermis thickness were measured using imageJ software program. Toluidine blue staining was used to count infiltrated mast cells. Briefly, hydrated tissue sections were stained with 0.1% Toluidine Blue O in 1% sodium chloride solution (pH 2; Sigma, USA) for 1 min. After staining, sections were washed briefly in PBS, and dehydration 3 times with 95% to 100% ethanol, and then sealed using mounting medium[35]. Sirius Red staining was used to count the number of infiltrated eosinophil cells[36]. Reagent preparation and staining protocol were according to previously as described[37].

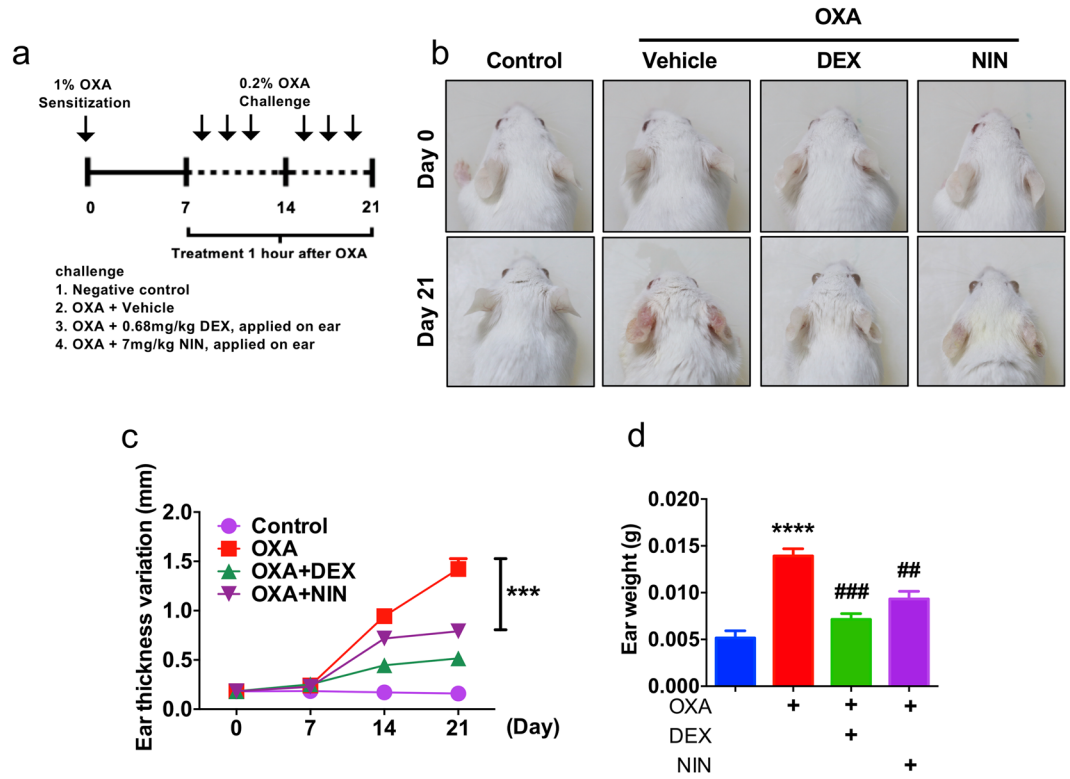

Figure 2. Morphological analysis of nintedanib-treated mice. (**a**) Schematic diagram of oxazolone (OXA)-induced animal model. Four groups: untreated controls, OXA only and mice treated with DEX (Dexamethasone) or nintedanib (NIN) one hour after every OXA challenge. (**b**) Representative photographs of mouse ears from each group on day 0 and 21. (**c**) Ear thickness was measured every week as indicated. Data are from three independent experiments (n = 15). Data are presented as mean ± SEM. Data (Day 21) are analyzed by student t-test. ***$p < 0.005$ compared to oxazolone treated. (**d**) Ear weight was measured at day 21. Data are from three independent experiments (n = 15). Data are presented as mean ± SEM and analyzed by one-way ANOVA (****$p < 0.001$ compared to control, $^{\#\#}p < 0.01$, $^{\#\#\#}p < 0.005$ compared to oxazolone treated).

Cells and reagents. NIH3T3/NKκB-luc cell line was purchased from Panomics (RC0015). Cells were maintained in a humidified incubator at 37 °C and 5% CO_2. FBM™-2 Fibroblast Growth Medium-2 BulletKit™ was purchased from Lonza (CC-3132, Lonza). Recombinant Human TNF-alpha was purchased from Peprotech (300-01A-10, Peprotech). Bay was purchased from Sigma (11-7082, Sigma). Nintedanib was purchased from Cayman chemical (11022).

Cell viability assay. Viability was performed as previously described with slight modification[38]. Briefly, 1×10^4 cells were plated in a 96 well plate. Pre-incubate the plate for 24 h in a humidified incubator. After nintedanib treatment, cells were incubated with mixture (1:10) of EZ-Cytox cell viability assay kit (Dogen, EZ3000). Then plate was incubated for 30 min in the incubator and determined absorbance at 450 nm with reference to 655 nm wavelength (iMark, Biorad).

Luciferase assay. Luciferase assay was performed as previously described with slight modification[39]. 6×10^5 cells were seeded in 24-well plates treated 50 nM TNF-α for 8 h with or without nintedanib. Cells were harvested and cell extracts were prepared using 100 µl of passive lysis buffer (Promega). Luciferase activities were measured using Veritas Luminometer (Turnur Designs, Sunnyvale, CA, USA).

Web-based meta-analysis. Microarray datasets from studies (GSE60028[40], GSE79150[41], GSE36842[42], GSE46239, GSE32924[43], GSE121212[44], GSE16161[45], GSE120721[46] and GSE107361[47] were analyzed using GEO2R (https://www.ncbi.nlm.nih.gov/geo/geo2r) to determine enzyme expression of RTK.

Serum IgE ELISA. Serum was collected from the abdominal aorta of mice. Whole blood was placed during 30 min at room temperature and centrifuged at 4 °C for 15 min at ×12,000 rpm. The supernatant was stored immediately at −80 °C. For analysis, samples were diluted to 1/200 with assay diluent. Total IgE were determined by ELISA kit according to manufacturer's manual (BD Pharmingen; San Diego, CA, USA). All measurements were analyzed by optical density at 450 nm.

RNA isolation and RT-PCR. Mice ear was homogenized in 1 ml of TRIzol reagent (Takara Co., Ltd. Japan) using IKA-T10 basic homogenizer (ULTRA-TURRAX; 10 mm; IKA Laboratory Equipment, Staufen, Germany). Total RNA was isolated previously described[48]. Total RNA was quantified by MaestroNano Micro-Volume

Spectrophotometer (Xiangshan Diist, Taiwan) and 300 ng RNA was used for reverse transcription using M-MLV reverse transcriptase (Invitrogen, California, USA). Real-time PCR analysis was performed with duplicate using SYBR® Master Mix in the BIOER Real-Time PCR machine (Fluorescent Quantitative Detection systems; Hangzhou, China). For calculation efficiency of the amplification, the relative quantitative of each target gene was normalized to the housekeeping gene as β-Actin. Data was calculated by the $2^{-\Delta\Delta CT}$ method based on the normalization gene of control group.

Immunofluorescence. Immunofluorescence was performed using a heat-induced epitope retrieval (HIER) protocol with slight modification[49]. After deparaffinization, slides were placed in a plastic container filled with citrate buffer, pH 6.0 at 60 °C for 20 min. And then, slides were allowed to cool for 20 min at room temperature and were then rinsed with phosphate-buffered saline with Tween 20 (PBST, Duchefa Biochemie, Hofmanweg, Netherlands). Slides were incubated in blocking buffer (BLOXALL® Endogenous Peroxidase and Alkaline Phosphatase Blocking Solution, Vector Laboratories, Inc., California, USA) for 1 h at room temperature to remove non-specific binding. Next, they were incubated for 24 h with Flt1 (VEGFR1) antibody (Santacruz biotechnology, Texas, USA) in blocking buffer at 4 °C. Next day, the slides were washed and incubated for 1 h at room temperature with anti-mouse secondary antibodies conjugated with Alexa Flour 647 (Abcam, Cambridge, United Kingdom). The slides were counterstained with DAPI for 10 min and mounted with fluorescence mounting medium (Agilent, California, USA).

Statistical analysis. All statistical evaluations were performed using Prism 6 (GraphPad Software, La Jolla, CA). Data are given as mean ± standard error of the mean (SEM). Statistical significance was analyzed using Student's *t*-test and one-way ANOVA. *P* values of <0.05, <0.01 and <0.001 were considered as statistically significant differences.

Ethics approval and consent to participate. All animals were care for by using protocols approved by the Institutional Animal Care and Use Committee (Konkuk University, Republic of Korea). No. KU10160.

Results

Vascular endothelial growth factor receptor1 (VEGFR1) is highly expressed in atopic dermatitis lesion. We determined the levels of RTKs (VEGFR1, PDGFRB and FGFR2) from dermatitis patients and normal controls using meta-analyses. Interestingly, the expression levels of VEGFR1 were increased from ten studies from seven independent datasets of lesion from dermatitis patients compared with control subjects (Fig. 1a and. Table S1) (GSE60028[40], GSE79150[41], GSE36842[42], GSE46239, GSE32924[43], GSE121212[44], GSE16161[45]). We found PDGFRB and FGFR2 were increased from dermatitis patients compared to normal control (Table S1). Moreover, we found the levels of VEGFR1 are increased in oxazolone (OXA) treated mice (Fig. 1b). Consequently, VEGFR1 was increased by infiltrated cells in dermis of OXA treated mice (Fig. 1c,d). These results indicated that expression of RTKs, especially VEGFR1 is increased in dermis of atopic dermatitis lesion.

Nintedanib ameliorates dermatitis in OXA-induced animal model. To determine whether nintedanib, RTK inhibitor is effective on dermatitis, we employed OXA-induced mice model (Fig. 2a). We found nintedanib treatment is able to attenuate morphological phenotype including skin redness and swelling of OXA-induced skin inflammation (Fig. 2b). Moreover, the levels of ear thickness and weight robustly decreased from mice cotreated with nintedanib and OXA compared to OXA-treated mice (Fig. 2c,d).

Nintedanib attenuates OXA-induced dermatitis in histological analysis. We found epidermis and dermis thickness are decreased from mice cotreated with nintedanib and OXA using histological analysis (Fig. 3a,b). Interestingly, numbers of infiltrated mast cells as well as eosinophils into dermis were decreased from mice cotreated with nintedanib and OXA compared to OXA-treated (Fig. 3d,e). Moreover, serum IgE levels were decreased from mice cotreated with nintedanib and OXA compared to OXA-treated mice (Fig. 3f). These results indicated that topical administration of nintedanib ameliorates OXA-induced dermatitis by histological analysis.

Nintedanib attenuates cytokine expression in OXA-induced model of dermatitis. Th2-type cytokines including IL-4 and IL-13 are one of the typical markers as well as therapeutic targets of atopic dermatitis[20]. We therefore, analyzed expression of cytokines from mice ear to determine whether nintedanib attenuates immune response. Interestingly, Th2 cytokines including IL-4, IL-5, IL-6, and IL-13 were decreased from mice cotreated nintedanib with OXA while there was no change on the expression of Th1 cytokines including TNF-α, IL-1β and IFN-γ (Fig. 4a–h). These results indicated that nintedanib attenuates Th2-type immune response in oxazolone-induced animal model of dermatitis. In order to determine the molecular mechanism of nintedanib-mediated anti-inflammatory effect, we used 3T3 murine fibroblasts, which stably expressed luciferase reporter plasmid encoded with NFκB-binding motif. Because 100 nM nintedanib-treated fibroblasts showed 91% viability, 50 nM and 100 nM nintedanib were used to measure NFκB activity in presence of TNF-α (Fig. S2a). We found that nintedanib is not able to modulate NFκB activity (Fig. S2b). These results indicated that NFκB may not be the primary molecular signaling pathway for nintedanib to inhibit oxazolone-induced animal model of dermatitis.

Discussion

We found the expression levels of RTKs especially, VEGFR are increased in the lesion of dermatitis patients (Fig. 1a and Table S1). There are numerous reports that VEGFR is highly expressed during inflammation and further studies are required to determine the role of VEGFR in lesion of dermatitis patients[50–52]. Moreover, systemic anti-VEGF treatments strongly reduced skin inflammation in a mice model of psoriasis[53]. Those observations

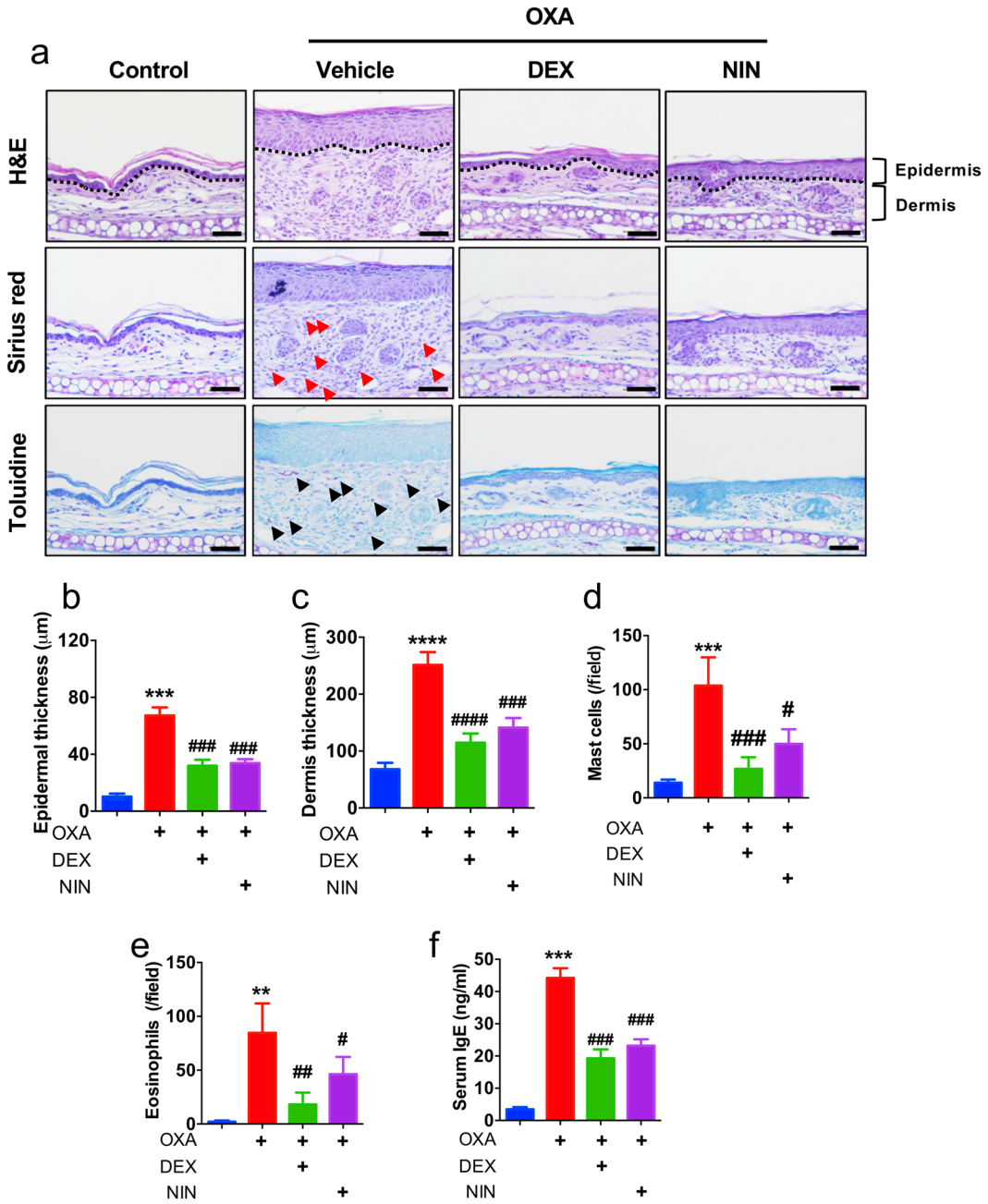

Figure 3. Histological analysis of nintedanib-treated mice. (**a**) H&E, sirius red and toluidine blue staining in ear lesions. Scale bar = 50 μm (**b**) Mean of epidermal thickness was measured using three different sections. (**c**) Mean of epidermal thickness was measured using three different sections. (**d**) Mean of mast cells (black arrow in toluidine blue staining) in dermis was measured. (**e**) Mean of eosinophil cells (red arrow in sirius red staining) in dermis was measured. (**f**) Serum IgE level was measured by ELISA at day 21. Data are from three independent experiments (n = 15). Data are presented as mean ± SEM of changes in values and analyzed by one-way ANOVA (**p < 0.01, ***p < 0.005, ****p < 0.001 compared to control, $^{\#}p < 0.05$, $^{\#\#}p < 0.01$, $^{\#\#\#}p < 0.005$, $^{\#\#\#\#}p < 0.001$ compared to oxazolone treated).

drove us to use nintedanib a potent FDA approved RTK inhibitor to determine therapeutic efficacy in animal model of dermatitis. We found that nintedanib treatment attenuates phenotype of oxazolone-induced skin inflammation in animal model without toxicity (Figs. 2b and S1). Histological analysis showed that nintedanib reduces infiltrated immune cells including mast cells and eosinophils (Fig. 3d,e). Moreover, the levels of Th2-type cytokines expression including IL-4 and IL-13 were reduced from nintedanib with OXA treated mice ear compared to OXA-treated (Fig. 4d-h). NFκB signaling is an important signaling pathway that orchestrates inflammatory response[54]. We found that nintedanib is not able to attenuate NFκB activity in presence of TNF-α (Fig. S2a,b). According to recent reports, nintedanib inhibits angiogenesis, reduced M (IL-4) cell polarization and induces apoptosis of mesenchymal cells during fibrotic remodeling[55–58]. Thus, we speculated that nintedanib

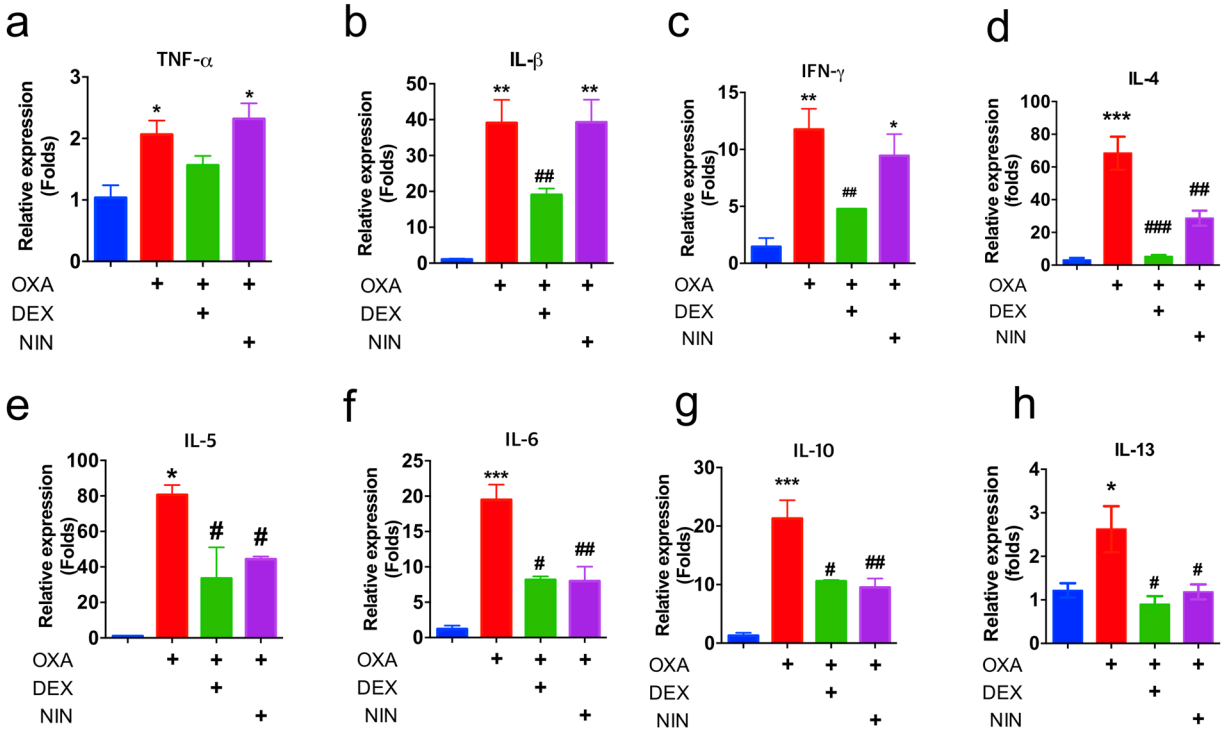

Figure 4. Expression of cytokines in nintedanib-treated mice. (**a**) mRNA levels of TNF-α from indicated mice ear. (**b**) mRNA levels of IL-β from indicated mice ear. (**c**) mRNA levels of IFN-γ from indicated mice ear. (**d**) mRNA levels of IL-4 from indicated mice ear. (**e**) mRNA levels of IL-5 from indicated mice ear. (**f**) mRNA levels of IL-6 from indicated mice ear. (**g**) mRNA levels of IL-10 from indicated mice ear. (**h**) mRNA levels of IL-13 from indicated mice ear. Data are from three independent experiments (n = 15). Data are presented as mean ± SEM and analyzed by one-way ANOVA (*$p < 0.05$, **$p < 0.01$, ***$p < 0.005$ versus control) and ($^{\#}p < 0.05$, $^{\#\#}p < 0.01$ versus OXA).

may regulate migration of inflammatory cells into the AD lesion by inhibiting angiogenesis, and/or immune cells polarization. Adverse effects of topical use of steroid-containing cream have been well established[59,60]. Although, novel drugs have been developed for dermatitis therapeutics including PDE4 inhibitors and JAK inhibitors, high costs of new drugs are one of the major burdens while dermatitis patients are increasing every year[61,62]. Therefore, repurposing drugs may cover these limitations of atopic dermatitis therapeutics. And nintedanib could be a one of the primary candidates as a repurposing drug because effects of nintedanib on air way inflammation is reported beyond current indication[63]. Future studies are remains to be explored to determine molecular mechanism of nintedanib-mediated anti-inflammatory effect on dermatitis.

Data availability

All study data are available from the corresponding author upon request.

Received: 7 November 2019; Accepted: 20 February 2020;
Published online: 11 March 2020

References

1. Lemmon, M. A. & Schlessinger, J. Cell signaling by receptor tyrosine kinases. *Cell* **141**, 1117–1134, https://doi.org/10.1016/j.cell.2010.06.011 (2010).
2. Schlessinger, J. Cell signaling by receptor tyrosine kinases. *Cell* **103**, 211–225, https://doi.org/10.1016/s0092-8674(00)00114-8 (2000).
3. Regad, T. & Targeting, R. T. K. Signaling Pathways in Cancer. *Cancers* **7**, 1758–1784, https://doi.org/10.3390/cancers7030860 (2015).
4. Szilveszter, K. P., Nemeth, T. & Mocsai, A. Tyrosine Kinases in Autoimmune and Inflammatory Skin Diseases. *Front. Immunol.* **10**, 1862, https://doi.org/10.3389/fimmu.2019.01862 (2019).
5. Mocsai, A., Kovacs, L. & Gergely, P. What is the future of targeted therapy in rheumatology: biologics or small molecules? *BMC Med.* **12**, 43, https://doi.org/10.1186/1741-7015-12-43 (2014).
6. Ghoreschi, K. & Gadina, M. Jakpot! New small molecules in autoimmune and inflammatory diseases. *Exp. Dermatol.* **23**, 7–11, https://doi.org/10.1111/exd.12265 (2014).
7. Virtanen, A. T., Haikarainen, T., Raivola, J. & Silvennoinen, O. Selective JAKinibs: Prospects in Inflammatory and Autoimmune Diseases. *BioDrugs* **33**, 15–32, https://doi.org/10.1007/s40259-019-00333-w (2019).
8. Bhagwat, S. S. Kinase inhibitors for the treatment of inflammatory and autoimmune disorders. *Purinergic Signal.* **5**, 107–115, https://doi.org/10.1007/s11302-008-9117-z (2009).
9. Pesu, M. *et al.* Therapeutic targeting of Janus kinases. *Immunol. Rev.* **223**, 132–142, https://doi.org/10.1111/j.1600-065X.2008.00644.x (2008).

10. Ghoreschi, K., Laurence, A. & O'Shea, J. J. Janus kinases in immune cell signaling. *Immunol. Rev.* **228**, 273–287, https://doi.org/10.1111/j.1600-065X.2008.00754.x (2009).
11. O'Shea, J. J., Kontzias, A., Yamaoka, K., Tanaka, Y. & Laurence, A. Janus kinase inhibitors in autoimmune diseases. *Ann. Rheum. Dis.* **72**(Suppl 2), ii111–115, https://doi.org/10.1136/annrheumdis-2012-202576 (2013).
12. Moran, N. Incyte comes of age with JAK inhibitor approval. *Nat. Biotechnol.* **30**, 3–5, https://doi.org/10.1038/nbt0112-3 (2012).
13. Leung, D. Y. New insights into atopic dermatitis: role of skin barrier and immune dysregulation. *Allergol. Int.* **62**, 151–161, https://doi.org/10.2332/allergolint.13-RAI-0564 (2013).
14. Ricci, G., Dondi, A., Patrizi, A. & Masi, M. Systemic therapy of atopic dermatitis in children. *Drugs* **69**, 297–306, https://doi.org/10.2165/00003495-200969030-00005 (2009).
15. Bieber, T. Atopic dermatitis. *N. Engl. J. Med.* **358**, 1483–1494, https://doi.org/10.1056/NEJMra074081 (2008).
16. David Boothe, W., Tarbox, J. A. & Tarbox, M. B. Atopic Dermatitis: Pathophysiology. *Adv. Exp. Med. Biol.* **1027**, 21–37, https://doi.org/10.1007/978-3-319-64804-0_3 (2017).
17. McPherson, T. Current Understanding in Pathogenesis of Atopic Dermatitis. *Indian. J. Dermatol.* **61**, 649–655, https://doi.org/10.4103/0019-5154.193674 (2016).
18. Hajar, T., Gontijo, J. R. V. & Hanifin, J. M. New and developing therapies for atopic dermatitis. *An. Bras. Dermatol.* **93**, 104–107, https://doi.org/10.1590/abd1806-4841.20187682 (2018).
19. Werfel, T. *et al.* Cellular and molecular immunologic mechanisms in patients with atopic dermatitis. *J. Allergy Clin. Immunol.* **138**, 336–349, https://doi.org/10.1016/j.jaci.2016.06.010 (2016).
20. Brunner, P. M., Guttman-Yassky, E. & Leung, D. Y. The immunology of atopic dermatitis and its reversibility with broad-spectrum and targeted therapies. *J. Allergy Clin. Immunol.* **139**, S65–S76, https://doi.org/10.1016/j.jaci.2017.01.011 (2017).
21. Stritesky, G. L. *et al.* The transcription factor STAT3 is required for T helper 2 cell development. *Immun.* **34**, 39–49, https://doi.org/10.1016/j.immuni.2010.12.013 (2011).
22. Takeda, K. *et al.* Essential role of Stat6 in IL-4 signalling. *Nat.* **380**, 627–630, https://doi.org/10.1038/380627a0 (1996).
23. Bao, L., Zhang, H. & Chan, L. S. The involvement of the JAK-STAT signaling pathway in chronic inflammatory skin disease atopic dermatitis. *JAKSTAT* **2**, e24137, https://doi.org/10.4161/jkst.24137 (2013).
24. Shibuya, M. Vascular Endothelial Growth Factor (VEGF) and Its Receptor (VEGFR) Signaling in Angiogenesis: A Crucial Target for Anti- and Pro-Angiogenic Therapies. *Genes. Cancer* **2**, 1097–1105, https://doi.org/10.1177/1947601911423031 (2011).
25. Koch, S. & Claesson-Welsh, L. Signal transduction by vascular endothelial growth factor receptors. *Cold Spring Harb. Perspect. Med.* **2**, a006502, https://doi.org/10.1101/cshperspect.a006502 (2012).
26. Agha-Majzoub, R., Becker, R. P., Schraufnagel, D. E. & Chan, L. S. Angiogenesis: the major abnormality of the keratin-14 IL-4 transgenic mouse model of atopic dermatitis. *Microcirculation* **12**, 455–476, https://doi.org/10.1080/10739680591003297 (2005).
27. Thomsen, S. F. Atopic dermatitis: natural history, diagnosis, and treatment. *ISRN Allergy* **2014**, 354250, https://doi.org/10.1155/2014/354250 (2014).
28. Koczy-Baron, E., Jochem, J. & Kasperska-Zajac, A. Increased plasma concentration of vascular endothelial growth factor in patients with atopic dermatitis and its relation to disease severity and platelet activation. *Inflamm. Res.* **61**, 1405–1409, https://doi.org/10.1007/s00011-012-0543-6 (2012).
29. Zhang, Y., Matsuo, H. & Morita, E. Increased production of vascular endothelial growth factor in the lesions of atopic dermatitis. *Arch. Dermatol. Res.* **297**, 425–429, https://doi.org/10.1007/s00403-006-0641-9 (2006).
30. Wollin, L. *et al.* Mode of action of nintedanib in the treatment of idiopathic pulmonary fibrosis. *Eur. Respir. J.* **45**, 1434–1445, https://doi.org/10.1183/09031936.00174914 (2015).
31. Keating, G. M. Nintedanib: A Review of Its Use in Patients with Idiopathic Pulmonary Fibrosis. *Drugs* **75**, 1131–1140, https://doi.org/10.1007/s40265-015-0418-6 (2015).
32. Lee, S. *et al.* Ameliorative effects of Juniperus rigida fruit on oxazolone- and 2,4-dinitrochlorobenzene-induced atopic dermatitis in mice. *J. Ethnopharmacol.* **214**, 160–167, https://doi.org/10.1016/j.jep.2017.12.022 (2018).
33. Choi, S. Y. *et al.* 2-deoxy-d-glucose Ameliorates Animal Models of Dermatitis. *Biomedicines* **8**, https://doi.org/10.3390/biomedicines8020020 (2020).
34. Jung, J. H., Wang, X. D. & Loeken, M. R. Mouse embryonic stem cells established in physiological-glucose media express the high KM Glut2 glucose transporter expressed by normal embryos. *Stem Cell Transl. Med.* **2**, 929–934, https://doi.org/10.5966/sctm.2013-0093 (2013).
35. Oishi, N. *et al.* Expression of precipitating factors of pruritus found in humans in an imiquimod-induced psoriasis mouse model. *Heliyon* **5**, e01981, https://doi.org/10.1016/j.heliyon.2019.e01981 (2019).
36. Meyerholz, D. K., Griffin, M. A., Castilow, E. M. & Varga, S. M. Comparison of histochemical methods for murine eosinophil detection in an RSV vaccine-enhanced inflammation model. *Toxicol. Pathol.* **37**, 249–255, https://doi.org/10.1177/0192623308329342 (2009).
37. Schmitz, N., Laverty, S., Kraus, V. B. & Aigner, T. Basic methods in histopathology of joint tissues. *Osteoarthr. Cartil.* **18**(Suppl 3), S113–116, https://doi.org/10.1016/j.joca.2010.05.026 (2010).
38. Jung, J. H. *et al.* Triad 1 induces apoptosis by p53 activation. *FEBS Lett.* **584**, 1565–1570, https://doi.org/10.1016/j.febslet.2010.03.011 (2010).
39. Jung, J. H. *et al.* E3 ubiquitin ligase Hades negatively regulates the exonuclear function of p53. *Cell Death Differ.* **18**, 1865–1875, https://doi.org/10.1038/cdd.2011.57 (2011).
40. Dhingra, N. *et al.* Molecular profiling of contact dermatitis skin identifies allergen-dependent differences in immune response. *J. Allergy Clin. Immunol.* **134**, 362–372, https://doi.org/10.1016/j.jaci.2014.03.009 (2014).
41. Blok, J. L., Li, K., Brodmerkel, C., Jonkman, M. F. & Horvath, B. Gene expression profiling of skin and blood in hidradenitis suppurativa. *Br. J. Dermatol.* **174**, 1392–1394, https://doi.org/10.1111/bjd.14371 (2016).
42. Gittler, J. K. *et al.* Progressive activation of T(H)2/T(H)22 cytokines and selective epidermal proteins characterizes acute and chronic atopic dermatitis. *J. Allergy Clin. Immunol.* **130**, 1344–1354, https://doi.org/10.1016/j.jaci.2012.07.012 (2012).
43. Suarez-Farinas, M. *et al.* Nonlesional atopic dermatitis skin is characterized by broad terminal differentiation defects and variable immune abnormalities. *J. Allergy Clin. Immunol.* **127**(954–964), e951–954, https://doi.org/10.1016/j.jaci.2010.12.1124 (2011).
44. Tsoi, L. C. *et al.* Atopic Dermatitis Is an IL-13-Dominant Disease with Greater Molecular Heterogeneity Compared to Psoriasis. *J. Invest. Dermatol.* **139**, 1480–1489, https://doi.org/10.1016/j.jid.2018.12.018 (2019).
45. Guttman-Yassky, E. *et al.* Broad defects in epidermal cornification in atopic dermatitis identified through genomic analysis. *J. Allergy Clin. Immunol.* **124**, 1235–1244 e1258, https://doi.org/10.1016/j.jaci.2009.09.031 (2009).
46. Esaki, H. *et al.* Identification of novel immune and barrier genes in atopic dermatitis by means of laser capture microdissection. *J. Allergy Clin. Immunol.* **135**, 153–163, https://doi.org/10.1016/j.jaci.2014.10.037 (2015).
47. Brunner, P. M. *et al.* Early-onset pediatric atopic dermatitis is characterized by TH2/TH17/TH22-centered inflammation and lipid alterations. *J. Allergy Clin. Immunol.* **141**, 2094–2106, https://doi.org/10.1016/j.jaci.2018.02.040 (2018).
48. Choi, Y. M., An, S., Bae, S. & Jung, J. H. Mdm2 is required for HDAC3 monoubiquitination and stability. *Biochem. Biophys. Res. Commun.* **517**, 353–358, https://doi.org/10.1016/j.bbrc.2019.07.052 (2019).
49. Parra, E. R. *et al.* Validation of multiplex immunofluorescence panels using multispectral microscopy for immune-profiling of formalin-fixed and paraffin-embedded human tumor tissues. *Sci. Rep.* **7**, 13380, https://doi.org/10.1038/s41598-017-13942-8 (2017).

50. Waldner, M. J. *et al*. VEGF receptor signaling links inflammation and tumorigenesis in colitis-associated cancer. *J. Exp. Med.* **207**, 2855–2868, https://doi.org/10.1084/jem.20100438 (2010).
51. Angelo, L. S. & Kurzrock, R. Vascular endothelial growth factor and its relationship to inflammatory mediators. *Clin. Cancer Res.* **13**, 2825–2830, https://doi.org/10.1158/1078-0432.CCR-06-2416 (2007).
52. Huggenberger, R. *et al*. Stimulation of lymphangiogenesis via VEGFR-3 inhibits chronic skin inflammation. *J. Exp. Med.* **207**, 2255–2269, https://doi.org/10.1084/jem.20100559 (2010).
53. Schonthaler, H. B., Huggenberger, R., Wculek, S. K., Detmar, M. & Wagner, E. F. Systemic anti-VEGF treatment strongly reduces skin inflammation in a mouse model of psoriasis. *Proc. Natl Acad. Sci. USA* **106**, 21264–21269, https://doi.org/10.1073/pnas.0907550106 (2009).
54. Liu, T., Zhang, L., Joo, D. & Sun, S. C. NF-kappaB signaling in inflammation. *Signal Transduct Target Ther* **2**, https://doi.org/10.1038/sigtrans.2017.23 (2017).
55. Cipriani, P. *et al*. Differential expression of stromal cell-derived factor 1 and its receptor CXCR4 in the skin and endothelial cells of systemic sclerosis patients: Pathogenetic implications. *Arthritis Rheum.* **54**, 3022–3033, https://doi.org/10.1002/art.22047 (2006).
56. da Silva, R. F. *et al*. Nintedanib antiangiogenic inhibitor effectiveness in delaying adenocarcinoma progression in Transgenic Adenocarcinoma of the Mouse Prostate (TRAMP). *J. Biomed. Sci.* **24**, 31, https://doi.org/10.1186/s12929-017-0334-z (2017).
57. Roth, G. J. *et al*. Nintedanib: from discovery to the clinic. *J. Med. Chem.* **58**, 1053–1063, https://doi.org/10.1021/jm501562a (2015).
58. Kasam, R. K., Reddy, G. B., Jegga, A. G. & Madala, S. K. Dysregulation of Mesenchymal Cell Survival Pathways in Severe Fibrotic Lung Disease: The Effect of Nintedanib Therapy. *Front. Pharmacol.* **10**, 532, https://doi.org/10.3389/fphar.2019.00532 (2019).
59. Fisher, D. A. Adverse effects of topical corticosteroid use. *West. J. Med.* **162**, 123–126 (1995).
60. Hengge, U. R., Ruzicka, T., Schwartz, R. A. & Cork, M. J. Adverse effects of topical glucocorticosteroids. *J Am Acad Dermatol* **54**, 1–15, quiz 16–18, https://doi.org/10.1016/j.jaad.2005.01.010 (2006).
61. Cotter, D. G., Schairer, D. & Eichenfield, L. Emerging therapies for atopic dermatitis: JAK inhibitors. *J. Am. Acad. Dermatol.* **78**, S53–S62, https://doi.org/10.1016/j.jaad.2017.12.019 (2018).
62. Clark, R. *et al*. Topical treatment utilization for patients with atopic dermatitis in the United States, and budget impact analysis of crisaborole ointment, 2. *J. Med. Econ.* **21**, 770–777, https://doi.org/10.1080/13696998.2018.1470520 (2018).
63. Lee, J. *et al*. Effect of nintedanib on airway inflammation in a mouse model of acute asthma. *J. Asthma* **57**, 11–20, https://doi.org/10.1080/02770903.2018.1544641 (2020).

Acknowledgements

We thank Na kyung Jeong for assisting mast cell count in histological analysis. This work is supported by the GeneCellPharm Corporation.

Author contributions

M.J.H., S.Y.C., C.M.L., Y.M.C. and J.H.J designed the experiments and analyzed the data. M.J.H., S.Y.C. and C.M.L. performed the experiments. M.J.H., J.H.J. and S.B. wrote the manuscript. S.A. and I.S.A. supported research grant.

Competing interests

The authors declare no competing interests.

Additional information

Supplementary information is available for this paper at https://doi.org/10.1038/s41598-020-61424-1.

Correspondence and requests for materials should be addressed to S.A. or J.H.J.

Reprints and permissions information is available at www.nature.com/reprints.

Publisher's note Springer Nature remains neutral with regard to jurisdictional claims in published maps and institutional affiliations.

Open Access This article is licensed under a Creative Commons Attribution 4.0 International License, which permits use, sharing, adaptation, distribution and reproduction in any medium or format, as long as you give appropriate credit to the original author(s) and the source, provide a link to the Creative Commons license, and indicate if changes were made. The images or other third party material in this article are included in the article's Creative Commons license, unless indicated otherwise in a credit line to the material. If material is not included in the article's Creative Commons license and your intended use is not permitted by statutory regulation or exceeds the permitted use, you will need to obtain permission directly from the copyright holder. To view a copy of this license, visit http://creativecommons.org/licenses/by/4.0/.

© The Author(s) 2020